scientific reports

Check for updates

OPEN

Effect of halogen substitution on the electronic and optical behavior of $C_{16}H_{10}X_2O_2$(X = F, cl, Br and I) organic semiconductors

F. Benlakhdar[1], M. A. Ghebouli[2,3], M. Fatmi[2]✉, B. Ghebouli[4], S. Alomairy[5], Faisal Katib Alanazi[6]✉, A. Djemli[7,8] & Talal M. Althagafi[5]

In this study, a comprehensive analysis of the structural, electronic, and optical properties of $C_{16}H_{10}X_2O_2$ compounds (where X = F, Cl, Br, I) was conducted using first-principles calculations based on Density Functional Theory (DFT). The results demonstrate that the substitution of different halogens significantly influences the electronic structure and optical properties of these organic compounds. Structural data revealed a systematic relationship between crystal lattice constants and the atomic radius and electronegativity of the substituted halogen atoms, with an observed increase in the c/a and c/b ratios when moving from F to I. Electronic band structure analysis showed that the band gap follows the pattern Br < Cl < F < I, indicating that brominated derivatives exhibit more pronounced semiconducting behavior. Partial Density of States (PDOS) curves confirm the pivotal role of halogen p orbitals in determining the properties of upper valence bands. Regarding optical properties, reflectivity, absorption, refractive index, and loss function spectra were analyzed across an energy range of 0–40 eV, revealing systematic variations correlated with the type of halogen substituent. Chlorine-containing compounds exhibited the highest reflectivity, absorption, and loss function values in the 15–25 eV range, while iodine-containing compounds showed the highest refractive index in the low-energy region. These structure-property relationships provide valuable insights for designing organic materials with specific electronic and optical properties for advanced organic electronics applications.

Keywords Halogenated organic semiconductors, Refractive index, Loss function, Structure-property relationships, $C_{16}H_{10}X_2O_2$, PDOS, TDOS, Optoelectronic materials

Organic semiconductors have emerged as promising materials for a wide range of electronic applications, including organic light-emitting diodes (OLEDs), organic solar cells (OSCs), and organic field-effect transistors (OFETs) due to their flexibility, low cost, and tunable electronic properties[1–3]. The ability to precisely engineer the electronic and optical properties of these materials represents a critical advantage over traditional inorganic semiconductors[4,5]. The field of organic electronics has witnessed remarkable growth over the past few decades, driven by the demand for lightweight, flexible, and cost-effective electronic devices. Unlike their inorganic counterparts, organic semiconductors offer several unique advantages, including solution processability, mechanical flexibility, and the potential for large-area fabrication through printing techniques. These attributes make them particularly attractive for applications in flexible displays, wearable electronics, and building-integrated photovoltaics[6,7]. The performance of organic electronic devices critically depends on the electronic and optical properties of the organic semiconducting materials. These properties are determined by the molecular structure,

[1]Research Center in Industrial Technologies CRTI, P.O. Box 64, Cheraga, Algiers 16014, Algeria. [2]Research Unit on Emerging Materials (RUEM), University Ferhat Abbas of Setif 1, Setif 19000, Algeria. [3]Department of Chemistry, Faculty of Sciences, University of M'sila University, Pole, Road BourdjBouArreiridj, 28000 msila, Algeria. [4]Laboratory of Studies Surfaces and Interfaces of Materials Solids (LESIMS), Faculty of Technology, University Ferhat Abbas of Setif 1, Setif 19000, Algeria. [5]Department of Physics, college of Sciences, Taif University, P.O. Box 11099, Taif 21944, Saudi Arabia. [6]Department of Physics, college of Sciences, Northern Border University, Arar 73222, Saudi Arabia. [7]Faculty of physics, University of Sciences & Technology Houari Boumediene (U.S.T.H.B), El Alia, BP 32, Bab Ezzouar, Algiers 16111, Algeria. [8]Physics and Chemistry of Materials Lab, Department of Physics, University of M'sila University, Pole, Road BourdjBouArreiridj, 28000 msila, Algeria. ✉email: ; Faisal.katib.al@gmail.com

which influences the intermolecular interactions, charge transport pathways, and light-matter interactions[8]. Among various strategies for molecular design, the incorporation of heteroatoms and functional groups has proven to be a powerful approach to tune the electronic properties of organic semiconductors[9].Halogenations has proven to be a particularly effective strategy for tuning the properties of organic semiconductors. The incorporation of halogen atoms can significantly alter the electronic structure, molecular packing, and frontier orbital energies of organic compounds[9,10]. The electronegativity, size, and polarizability of different halogens provide a systematic means to manipulate the HOMO-LUMO gap, charge transport characteristics, and light absorption/emission properties[11,12]. The influence of halogen atoms on the properties of organic semiconductors operates through multiple mechanisms. First, halogens can modify the electronic structure through inductive effects, withdrawing electron density from the conjugated system and lowering the energy levels of both the highest occupied molecular orbital (HOMO) and the lowest unoccupied molecular orbital (LUMO)[13]. This effect is particularly pronounced for fluorine, which possesses the highest electronegativity among all elements. Second, halogens can participate in non-covalent interactions, such as halogen bonding and π-π interactions, which influence the molecular packing in the solid state and, consequently, the charge transport properties[14]. Third, the presence of heavy halogen atoms can enhance spin-orbit coupling, facilitating intersystem crossing and potentially improving the performance of OLEDs through increased phosphorescence[15].The systematic variation of halogen substituents offers a unique opportunity to establish structure-property relationships in organic semiconductors. By replacing one halogen atom with another while keeping the molecular scaffold unchanged, researchers can isolate the effects of electronegativity, atomic size, and polarizability on the electronic and optical properties[16].The study of electronic and optical properties of halogenated organic compounds is of significant importance for the development of effective materials for optoelectronic applications. Previous studies have indicated that substitution of different halogens in the molecular structure substantially influences the electronic gap and electron transport properties[17]. In this paper, we present a comprehensive investigation of the structural, electronic, and optical properties of $C_{16}H_{10}\times_2O_2$ compounds (where X = F, Cl, Br, and I). Through systematic first-principles calculations, we explore the profound effects of halogen substitution on these properties. This approach not only provides fundamental insights into the relationship between molecular structure and functional properties but also opens new avenues for designing organic materials with tailored characteristics for advanced optoelectronic applications. Our comparative analysis reveals how subtle atomic replacements within the molecular framework can significantly alter the electronic band structure, optical absorption, and ultimately the macroscopic behavior of these compounds.

Computational method

First-principle calculations were performed using the Cambridge Serial Total Energy (CASTEP) code[18]. The Kohn-Sham equations were solved within the framework of density functional theory (DFT)[19,20] by expanding the wave functions of valence electrons in a basis set of plane waves with kinetic energy smaller than a specified cut-off energy, Ecut. Integrations over the Brillouin zone were replaced by discrete summation over a special set of k-points using the Monkhorst-Pack scheme[21].A plane wave cut-off energy of 600 eV and an $8\times8\times8$ grid of Monkhorst-Pack points was employed in this study to ensure good convergence of the computed structures and energies. For the calculation of optical properties, which typically requires a dense mesh of uniformly distributed k-points, the Brillouin zone integration was performed using a $20\times20\times20$ grid of Monkhorst-Pack points. Density Functional Theory (DFT) calculations were performed using the Generalized Gradient Approximation (GGA) with the PBE functional to describe exchange-correlation interactions[22]. This methodology has been optimized for studying halogenated organic compounds as previous studies have demonstrated its good agreement with experimental results for electronic and optical properties[23]. The structural parameters of $C_{16}H_{10}\times_2O_2$ compounds (where X = F, Cl, Br, and I) were determined using the Broyden-Fletcher-Goldfarb-Shanno (BFGS) minimization technique[24], with the following thresholds for converged structures: energy change per atom less than 5×10^{-6} eV, residual force less than 0.01 eV/Å, stress below 0.03 GPa, and displacement of atoms during geometry optimization less than 0.0005 Å.The optical properties were derived from the complex dielectric function $\varepsilon(\omega)=\varepsilon_1(\omega)+i\varepsilon_2(\omega)$. The imaginary part was calculated from the momentum matrix elements between occupied and unoccupied wave functions within the selection rules. The real part of the dielectric function follows from the Kramer-Kronig relationship.

Results and discussion

Structural characterization

The crystal structures of the (2*E*)−1,4-bis(4-halophenyl)but-2-ene-1,4-dione compounds ($C_{16}H_{10}\times_2O_2$, where X = F, Cl, Br, I) were investigated using first-principles calculations based on density functional theory (DFT). These chalcone-like derivatives crystallize in the monoclinic space group $P2_1/c$ (No. 14) with Z = 2 formula units per unit cell. Figure 1; shows the molecular structure of the brominated compound (C16H10Br2O2) as a representative example of this family. The compounds $C_{16}H_{10}X_2O_2$ (X = F, Cl, Br, I) represent a series of halogenated derivatives whose crystal structures are notably influenced by the type of halogen. The systematic variation in the unit cell parameters correlates with the increasing atomic radius and decreasing electronegativity of the halogen atoms when moving from F to I. The optimized lattice parameters for all four compounds are summarized in Table 1,

The calculated data show a decrease in the lattice parameter *a* and an increase in *c* as the halogen atom becomes larger, indicating elongation along the c-axis. The ratios *c/a* and *c/b* also increase progressively from F to I. Among the studied derivatives, both the chlorinated and brominated compounds ($C_{16}H_{10}Cl_2O_2$ and $C_{16}H_{10}Br_2O_2$) were experimentally characterized by single-crystal X-ray diffraction[22], allowing direct comparison with the DFT-optimized structures. For the Cl compound, the experimental unit cell parameters

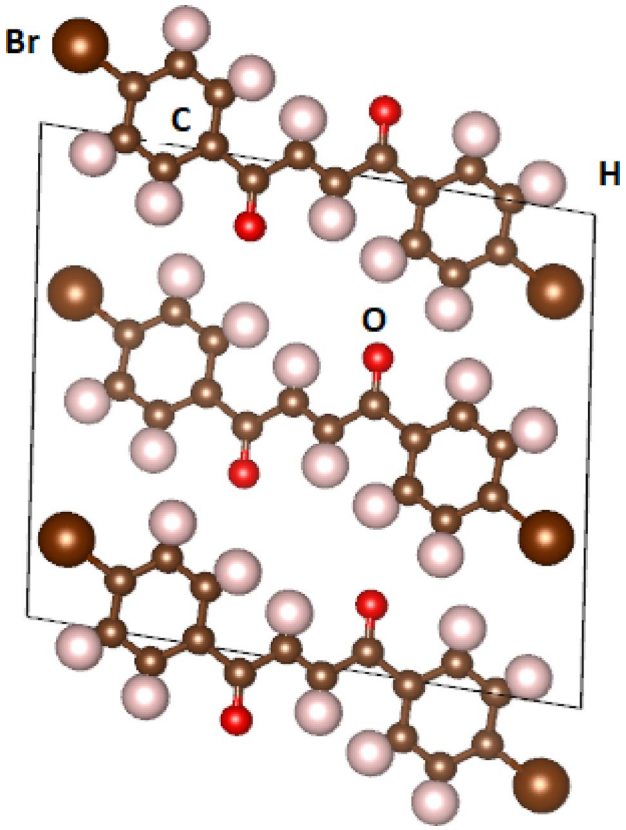

Fig. 1. Crystal structures of the (2*E*)−1,4-bis(4-halophenyl)but-2-ene-1,4-dione compounds ($C_{16}H_{10}Br_2O_2$).

X content	a (Å)	b (Å)	c (Å)	c/a	c/b
F	13,6186	6,89704	14,3305	1,0523	2,0778
Cl	12,6591	6,16199	13,4770	1,0646	2,1703
Br	12,3884	6,20970	13,5703	1,0954	2,1853
I	12,5424	6,19105	13,7288	1,0946	2,2175

Table 1. The calculated lattice parameters of the (2*E*)−1,4-bis(4-halophenyl)but-2-ene-1,4-dione compounds ($C_{16}H_{10}\times_2O_2X$=(F, cl, Br and I)).

are $a = 13.95$ Å, $b = 6.08$ Å, $c = 14.68$ Å, while the calculated values are $a = 12.66$ Å, $b = 6.16$ Å, $c = 13.48$ Å. For the Br compound, experimental parameters are $a = 14.44$ Å, $b = 5.99$ Å, $c = 12.72$ Å (monoclinic), compared to the computed ones: $a = 12.39$ Å, $b = 6.21$ Å, $c = 13.57$ Å. While some deviations exist—particularly in the *b*-axis—the calculated values generally reproduce the experimental trends in lattice expansion and symmetry. or the fluorinated and iodinated derivatives ($C_{16}H_{10}F_2O_2$ and $C_{16}H_{10}I_2O_2$), only theoretical data are currently available. However, based on the good agreement observed between DFT-calculated and experimentally determined lattice parameters for the chlorinated and brominated compounds, it is reasonable to assume that the predicted structures for the remaining derivatives are reliable and can serve as a solid reference for future experimental validation. The optimized lattice parameters for $C_{16}H_{10}F_2O_2$ are $a = 13.62$ Å, $b = 6.90$ Å, $c = 14.33$ Å, while those for $C_{16}H_{10}I_2O_2$ are $a = 12.54$ Å, $b = 6.19$ Å, $c = 13.73$ Å. These values reflect the expected structural trends across the halogen series, further supporting the consistency and predictive power of the DFT approach used in this study.

Electronic properties

Electronic structure

The electronic band structures of the compounds $C_{16}H_{10}X_2O_2$ (where X = F, Cl, Br, I) were calculated using DFT methods are show in Fig. 2, with the Fermi level set at 0 eV. These band structure diagrams provide insight into the effect of halogen substitution on the electronic properties of the studied molecules.In the band structure of $C_{16}H_{10}Br_2O_2$, a clear energy gap is observed between the valence and conduction bands, indicating semiconducting behavior. The bands are relatively closer around the Fermi level compared to the other halogenated compounds, suggesting that the presence of bromine atoms tends to narrow the band gap and

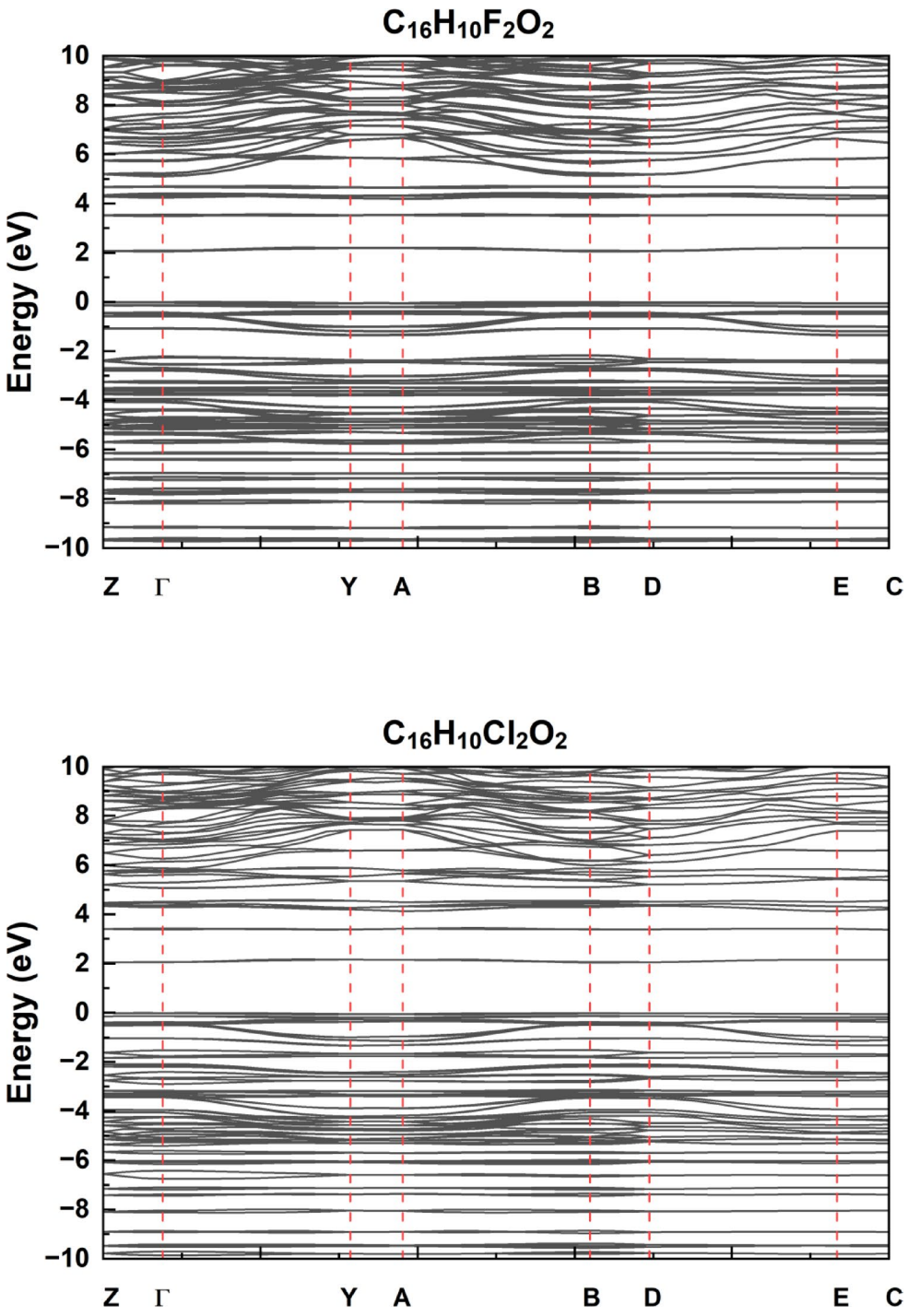

Fig. 2. Electronic Band Structure of for the $C_{16}H_{10}X_2O_2$ compounds (where X = F, Cl, Iand Br): High-Symmetry Path Analysis in Reciprocal Space.

enhance electronic conductivity.The structure for $C_{16}H_{10}I_2O_2$ shows a wider band gap, implying more insulating behavior. This can be attributed to the larger atomic radius of iodine, which reduces orbital overlap and weakens electronic interactions, increasing the energy separation between bands.In $C_{16}H_{10}Cl_2O_2$, the band gap lies between those of the brominated and iodinated analogues, implying that chlorine has a more balanced effect. It provides moderate orbital overlap, resulting in intermediate semiconducting behavior.The band structure of $C_{16}H_{10}F_2O_2$ exhibits a distinct trend. Due to the high electronegativity and small atomic radius of fluorine, there is stronger localization of electrons, which leads to a more rigid band structure and a relatively wider band gap compared to Br and Cl, though slightly narrower than that of I. This suggests that fluorine substitution contributes to enhanced electronic stability but at the cost of reduced conductivity.Overall, the results clearly demonstrate that halogen substitution significantly modulates the band gap and, consequently, the electronic

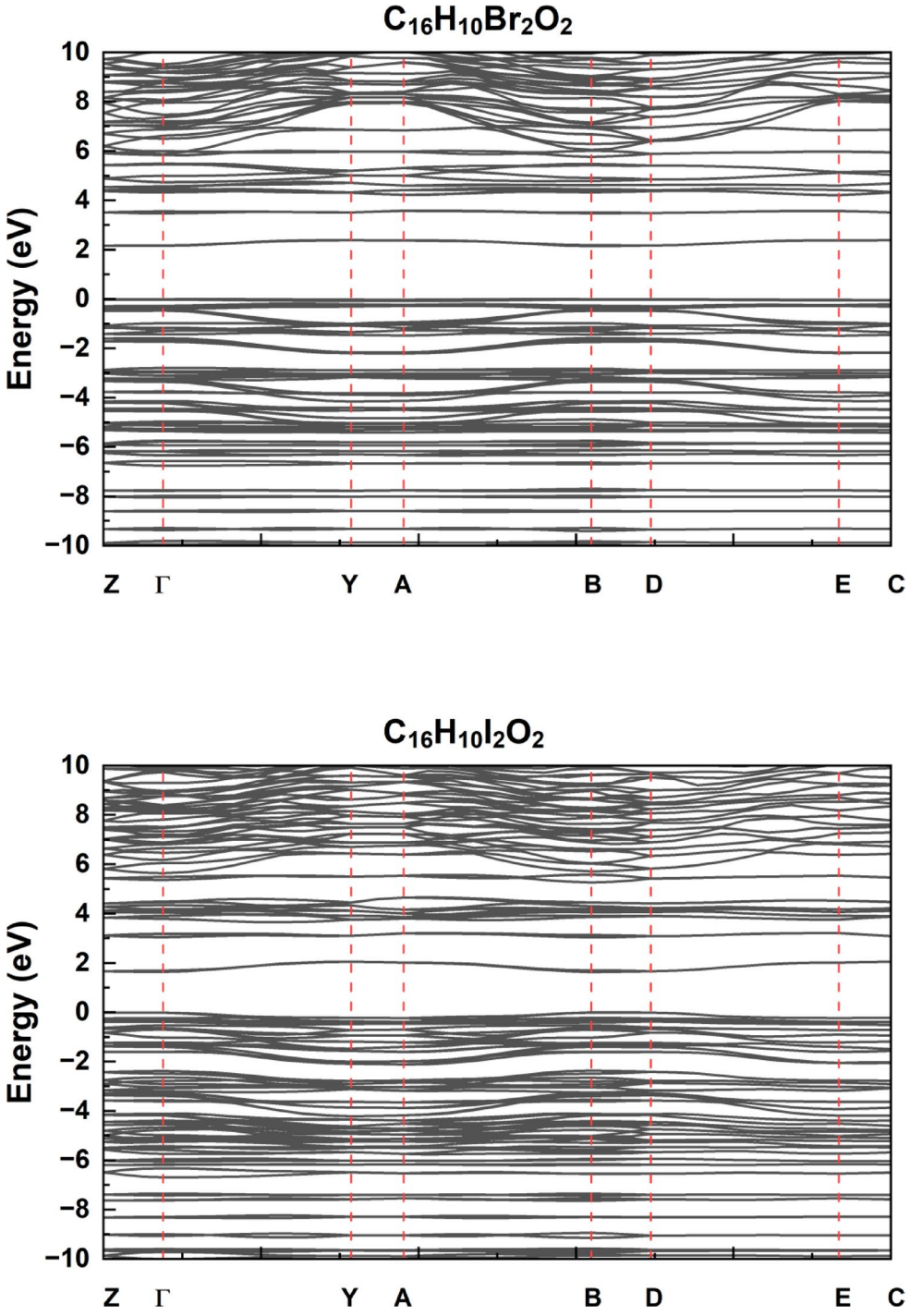

Fig. 2. (continued)

behavior of the $C_{16}H_{10}X_2O_2$ series. The calculated band gaps for the $C_{16}H_{10}X_2O_2$ compounds follow the trend: **I < Cl < F < Br**, with iodine-substituted molecules exhibiting the narrowest band gap (1.63 eV), and brominated ones the widest (2.15 eV). This indicates that the incorporation of heavier halogens, particularly iodine, enhances the semiconducting behavior by narrowing the energy gap. The calculated energy band gaps for each compound are summarized in Table 2, highlighting the progressive variation across the halogen series.

Density of state

As shown in Fig. 3, analysis of the Partial Density of States (PDOS) and Total Density of States (TDOS) curves for the $C_{16}H_{10}Br_2O_2$ compound reveals a distinctive distribution of electronic properties across the energy range from − 10 to + 10 eV. These curves expose a complex electronic structure where C (p) orbitals contribute predominantly to the density of states, with prominent peaks at −6, −4, and − 2 eV in the valence band region

Compound	Band Gap (eV)
$C_{16}H_{10}F_2O_2$	2.06
$C_{16}H_{10}Cl_2O_2$	2.04
$C_{16}H_{10}Br_2O_2$	2.15
$C_{16}H_{10}I_2O_2$	1.63

Table 2. Calculated energy band gaps (in eV) of $C_{16}H_{10}X_2O_2$ compounds with different halogen substituents (X = F, cl, br, I).

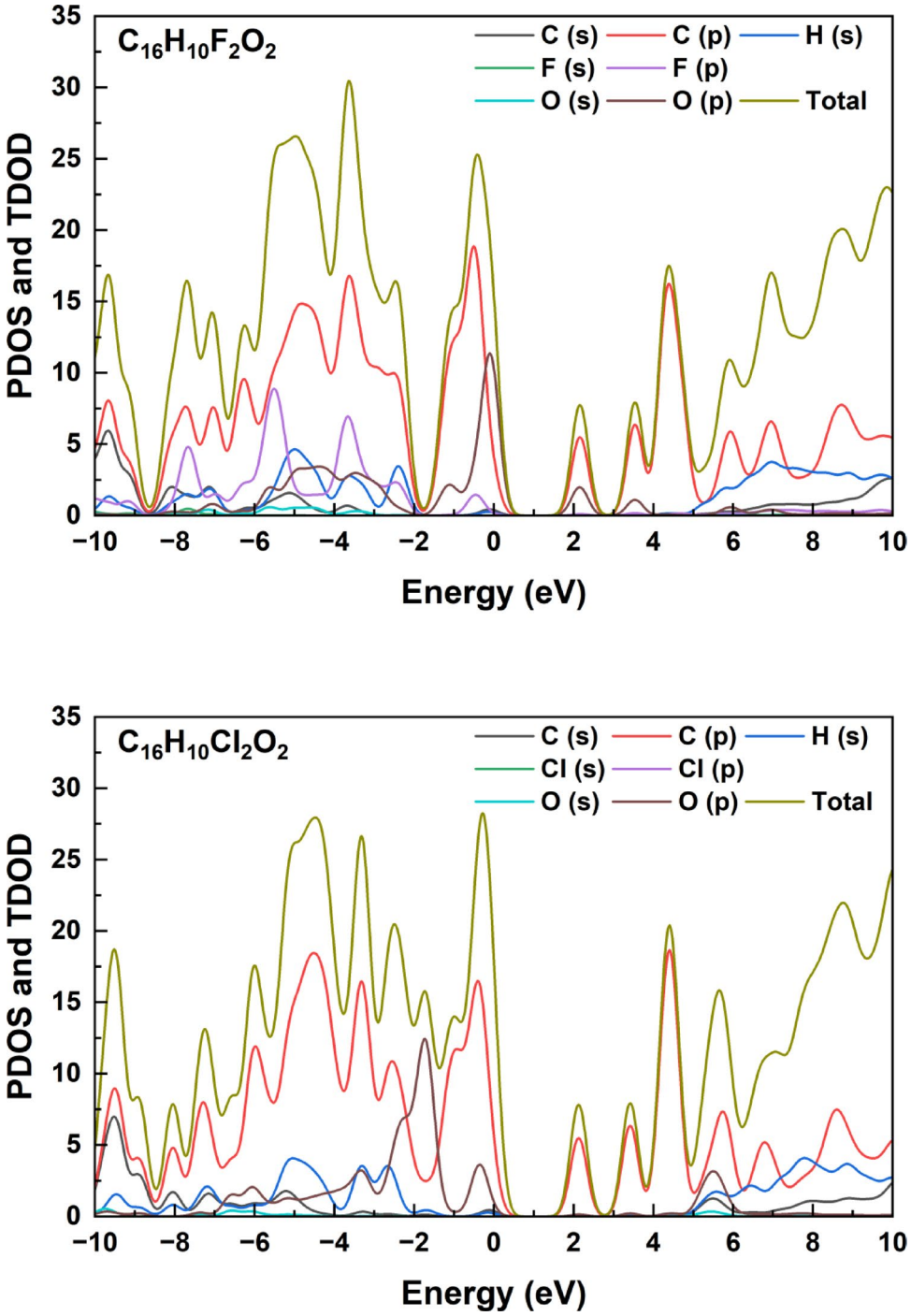

Fig. 3. Partial Density of States (PDOS) and Total Density of States (TDOS) curves for the $C_{16}H_{10}X_2O_2$ compounds (where X = F, Cl, Iand Br).

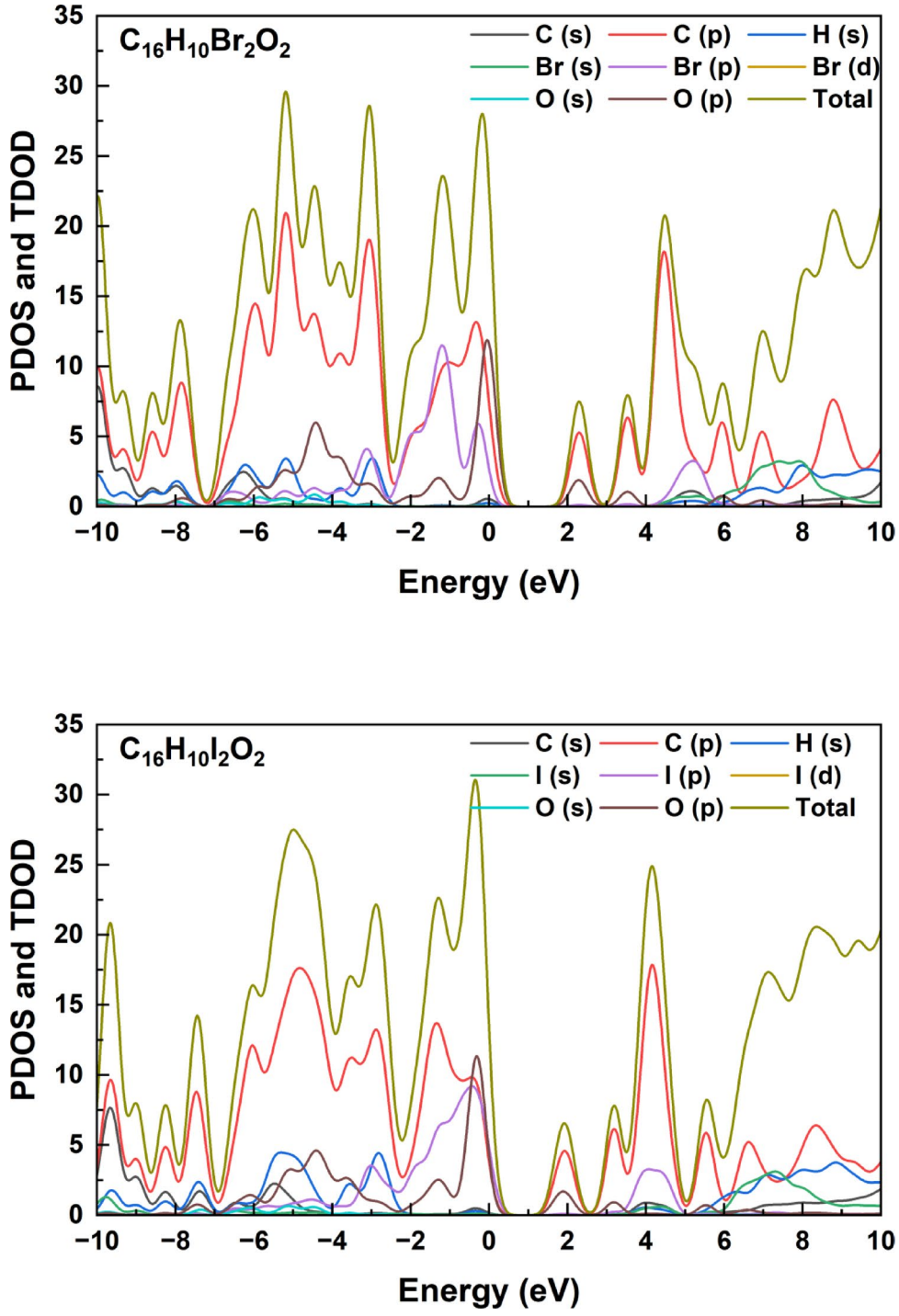

Fig. 3. (continued)

(negative energy). The contribution of Br (p) orbitals is clearly visible in Fig. 3, especially in the range from −2 to 0 eV, while hydrogen and oxygen contributions remain relatively minor. The curves indicate the presence of an energy gap around the Fermi level (0 eV), separating the electron-occupied valence bands from the unoccupied conduction bands. In the positive energy region, a prominent peak appears at approximately + 4 eV with significant contribution from C (p) orbitals, while the TDOS curve (yellow line) continues to rise beyond + 6 eV. Comparing these results with similar $C_{16}H_{10}X_2O_2$ compounds (where X = F, Cl, I) suggests that halogen substitution slightly affects the density of states distribution, with differences in curve shapes and peak heights, particularly in regions close to the Fermi level. These electronic characteristics play a pivotal role in determining the physical and chemical behavior of the compound, including electrical conductivity, optical absorption, and chemical reactivity properties.The PDOS curves presented in this study show a pattern similar to that found

by Lee et al. in their study of halogenated organic derivatives, where halogen p orbitals play a pivotal role in determining the properties of upper valence bands, affecting the electronic gap and electron transitions[25].

Optical properties

Reflectivity

The reflectivity spectra of $C_{16}H_{10}X_2O_2$ compounds containing halogen atoms (X = F, Cl, Br, I), as shown in Fig. 4, display distinct optical behavior across a broad spectral range from approximately 30 nm to 1200 nm. In the short-wavelength region (30–400 nm), corresponding to the ultraviolet (UV) and vacuum ultraviolet (VUV) domains, sharp reflectivity peaks are observed for all compounds. These peaks are attributed to $\pi \rightarrow \pi^*$ and $\mathbf{n} \rightarrow \pi^*$ electronic transitions, as well as excitations from deep valence or semi-core states. The maximum reflectivity is recorded around 50–100 nm, particularly for $C_{16}H_{10}Cl_2O_2$ and $C_{16}H_{10}I_2O_2$, suggesting a strong interaction between incident photons and localized electronic states. This behavior highlights the influence of halogen electronegativity and polarizability on the dielectric response of the materials. As the wavelength increases beyond 400 nm (visible range), reflectivity gradually decreases, consistent with a reduction in electronic excitations. The spectra begin to converge toward the upper end of the range, indicating similar optical responses among the compounds in the near-infrared (NIR) region. Among all compounds, $C_{16}H_{10}Cl_2O_2$ exhibits the highest reflectivity across most of the spectrum, while $C_{16}H_{10}F_2O_2$ shows the lowest, reinforcing the role of halogen substitution in tailoring the light–matter interaction in organic semiconductors.

Absorption

The absorption spectra of the halogenated organic compounds $C_{16}H_{10}X_2O_2$ (X = F, Cl, Br, I), now plotted as a function of wavelength (nm) (Fig. 5), demonstrate clear optical trends across a broad spectral range from 0 to 1200 nm. In the short-wavelength region (30–200 nm), corresponding to the vacuum ultraviolet (VUV) and deep ultraviolet (DUV), all compounds show sharp and intense absorption peaks. These features are attributed to $\pi \rightarrow \pi^*$ and $\mathbf{n} \rightarrow \pi^*$ electronic transitions and deep interband excitations within the valence band. The chlorinated compound ($C_{16}H_{10}Cl_2O_2$) exhibits the highest absorption peak, reaching nearly 280,000 units around 77.5 nm, while $C_{16}H_{10}F_2O_2$ shows a slightly blue-shifted maximum near 69 nm, indicating higher energy excitations. The brominated and iodinated compounds present similar spectral profiles, with broader peaks and slightly shifted absorption edges. Beyond 200 nm, all compounds show rapidly decreasing absorption, and approach near-zero values beyond 800–1000 nm, indicating negligible optical absorption in the near-infrared (NIR) region. These spectral variations clearly reflect the influence of halogen substitution on the electronic structure and light–matter interactions of the molecules. When compared to the reflectivity data, the **a**bsorption peaks generally correspond to minima or inflection points in reflectivity, highlighting the expected inverse relationship between the two properties in accordance with fundamental optical principles. The reflectivity and absorption spectra results align with the study by Yamamoto et *al.*[26] who demonstrated that halogen substitution in organic compounds leads to systematic changes in optical properties, particularly in the energy range of 15–25 eV which is associated with core-level transitions.

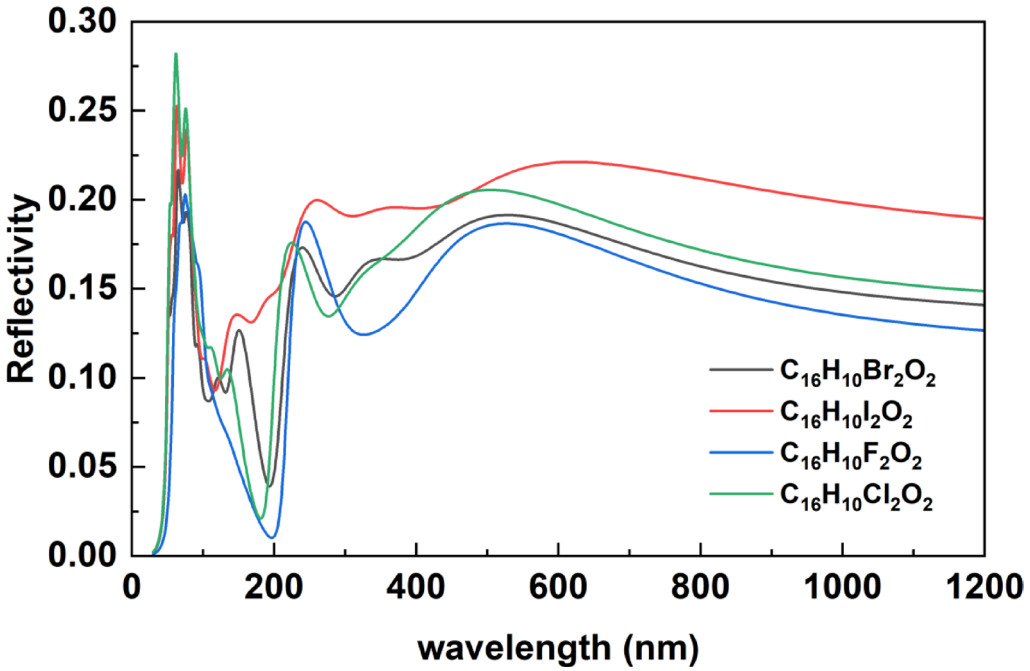

Fig. 4. Reflectivity Spectra of Halogenated $C_{16}H_{10}X_2O_2$ Compounds (X = F, Cl, Br, I).

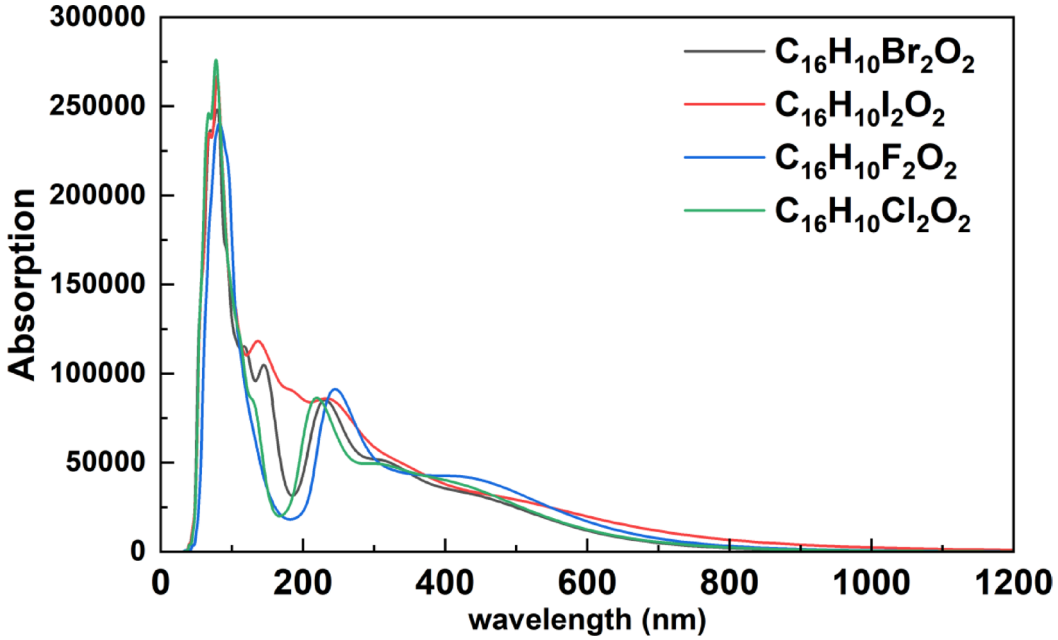

Fig. 5. Absorption Spectra of Halogenated $C_{16}H_{10}X_2O_2$ Compounds (X = F, Cl, Br, I).

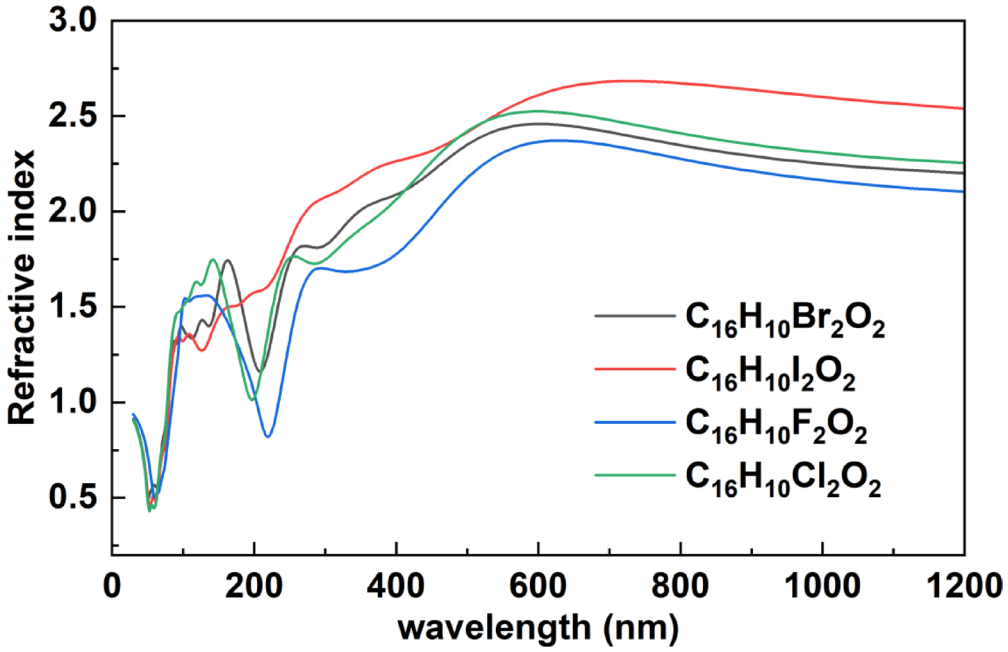

Fig. 6. The refractive index Spectra of Halogenated $C_{16}H_{10}X_2O_2$ Compounds (X = F, Cl, Br, I).

Refractive index

Figure 6, presents the refractive index spectra of the halogen-substituted organic compounds $C_{16}H_{10}X_2O_2$ (X = F, Cl, Br, I), plotted as a function of wavelength (nm) across the spectral range of 0 to 1200 nm. In the short-wavelength region (30–200 nm), which corresponds to the vacuum and deep ultraviolet, all compounds exhibit pronounced variations in refractive index. Clear peaks are observed between approximately 100–200 nm, reflecting the strong dispersion behavior due to electronic transitions in this high-energy region. As the wavelength increases toward the visible spectrum (400–700 nm), the refractive index begins to stabilize gradually. The compound $C_{16}H_{10}I_2O_2$ (iodine) shows the highest refractive index values in this range (~2.6–2.7), followed by $C_{16}H_{10}Br_2O_2$, $C_{16}H_{10}Cl_2O_2$, and finally $C_{16}H_{10}F_2O_2$. This trend correlates with the increasing atomic number and polarizability of the halogen atoms, where heavier halogens contribute more significantly to the material's optical response. In the near-infrared region (700–1200 nm), the refractive index curves become

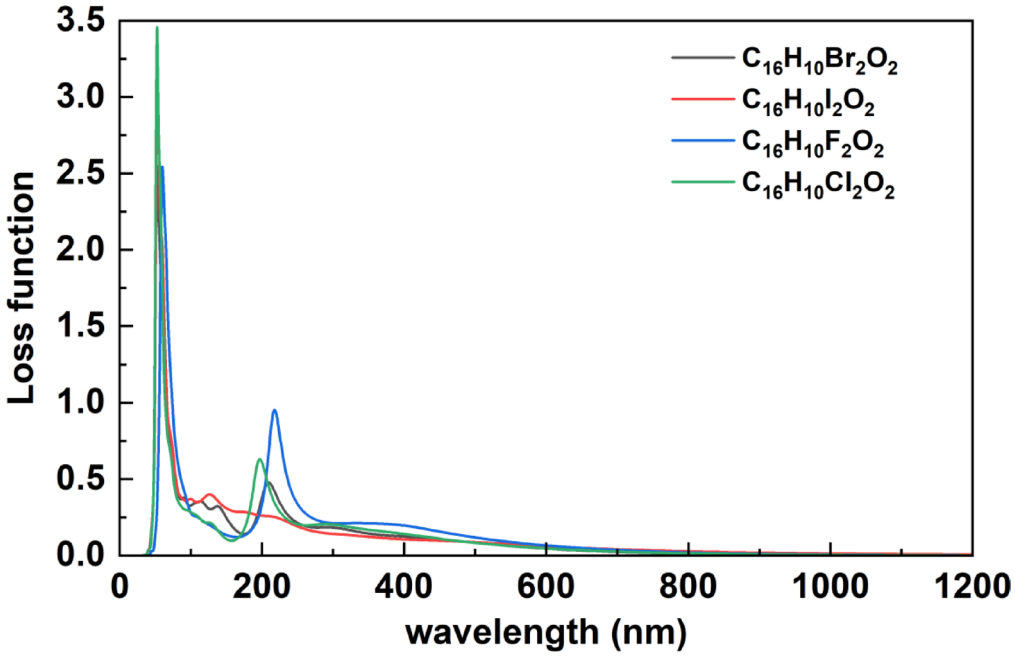

Fig. 7. Loss function Spectra of Halogenated $C_{16}H_{10}X_2O_2$ Compounds(X = F, Cl, Br, I).

nearly flat for all compounds, indicating a stable optical response and reduced dispersion as photon energy decreases. These observations are consistent with the earlier results from absorption and reflectivity spectra. The regions of high refractive index typically align with the onset of absorption or reflectivity features, supporting the underlying physical relationship described by the Kramers-Kronig relations. The systematic differences in optical response caused by halogen substitution offer valuable insights for tuning the electronic and optical properties of organic semiconductors. These findings suggest potential for the design of custom optical materials tailored for use in optoelectronic applications.

Loss function

Figure 7 shows the loss function spectra of the halogenated organic compounds $C_{16}H_{10}X_2O_2$ (X = F, Cl, Br, I), plotted as a function of wavelength (nm) across the spectral range of 0–1200 nm. The loss function represents the energy dissipation of fast electrons interacting with the material and provides insight into plasmonic resonances and electronic excitation mechanisms. All compounds exhibit a dominant peak at short wavelengths (~ 50–60 nm), which corresponds to high-energy plasmonic excitations typically occurring when the real part of the dielectric function approaches zero. Among the compounds, $C_{16}H_{10}Cl_2O_2$ shows the most intense peak (~ 3.4), followed by $C_{16}H_{10}I_2O_2$, $C_{16}H_{10}F_2O_2$, and $C_{16}H_{10}Br_2O_2$. These variations confirm the strong influence of the halogen atom on collective electronic behavior. A secondary feature appears around 150–200 nm, most clearly in $C_{16}H_{10}F_2O_2$, which indicates the presence of low-energy excitation modes such as interband transitions or possible surface plasmon activity. Beyond 300 nm, the loss function values decrease sharply and remain near zero throughout the visible and near-infrared regions, indicating minimal energy dissipation from collective excitations in these longer-wavelength ranges. These results are consistent with previously analyzed refractive index, reflectivity, and absorption spectra, reinforcing the relationship described by the Kramers-Kronig relations. Notably, the main plasmon resonance near 50–60 nm corresponds to wavelengths where the refractive index reaches its minimum and absorption is reduced, supporting the identification of strong collective electronic oscillations. The differences observed between halogenated compounds reflect the role of atomic polarizability and electronic structure in modulating energy loss behavior. The chlorinated derivative demonstrates the most prominent collective excitation, suggesting enhanced light-matter coupling due to the nature of the Cl atom. This wavelength-based analysis offers a comprehensive view of energy loss dynamics in these compounds and supports their potential for applications in plasmonic sensors, nanophotonics, and optical energy management, where control of energy dissipation is critical. The notable differences in the loss function spectra among different halogenated compounds align with findings by Zhang et *al.*[27] who demonstrated that the plasmonic response of organic compounds is significantly affected by the type of halogen substituent, with systematic changes in the intensity and position of collective excitation peaks.

Conclusion

In this study, a detailed first-principles investigation was carried out to explore the impact of halogen substitution on the structural, electronic, and optical properties of $C_{16}H_{10}X_2O_2$ compounds (where X = F, Cl, Br, I). The results clearly demonstrate that the type of halogen significantly alters the crystal lattice parameters, band gap, and optical response of these materials. A systematic trend was observed where increasing the halogen atomic

number led to a decrease in the band gap and distinct variations in reflectivity, absorption, refractive index, and energy loss spectra. These variations are directly linked to the halogens' electronegativity, atomic size, and polarizability, underscoring the effectiveness of halogenation as a strategy for tuning the functional properties of organic semiconductors. Notably, chlorinated compounds exhibited the most intense optical responses in the 15–25 eV range, while iodinated derivatives showed the highest refractive index at low photon energies. The comprehensive analysis presented in this work provides valuable insight into the structure-property relationships of halogenated organic materials, offering a predictive framework for the rational design of next-generation optoelectronic devices such as OLEDs, OFETs, and organic photovoltaics. Future experimental validation of the predicted properties, particularly for fluorinated and iodinated derivatives, will further enhance the development of tailored organic electronic materials.

Data availability

Data availability statement: Data underlying the results presented in this paper are not publicly available at this time but may be obtained from the corresponding author (fatmimessaud@yahoo.fr) upon reasonable request.

Received: 1 May 2025; Accepted: 14 July 2025
Published online: 17 July 2025

References

1. Forrest, S. R. The path to ubiquitous and low-cost organic electronic appliances on plastic. *Nature* **428**, 911–918 (2004).
2. Klauk, H. Organic thin-film transistors. *Chem. Soc. Rev.* **39** (7), 2643–2666 (2006).
3. Brabec, C. J., Sariciftci, N. S. & Hummelen, J. C. Plastic solar cells. *Adv. Funct. Mater.* **11** (1), 15–26 (2001).
4. Zaumseil, J. & Sirringhaus, H. Electron and ambipolar transport in organic field-effect transistors. *Chem. Rev.* **107** (4), 1296–1323 (2007).
5. Günes, S., Neugebauer, H. & Sariciftci, N. S. Conjugated polymer-based organic solar cells. *Chem. Rev.* **107** (4), 1324–1338 (2007).
6. Wang, S., Ha, M., Manno, M., Daniel Frisbie, C. & Leighton, C. Hopping transport and the hall effect near the insulator–metal transition in electrochemically doped polythiophene. *Nat. Commun.* **10**, 3623 (2019).
7. Root, S. E., Savagatrup, S., Printz, A. D., Rodriquez, D. & Lipomi, D. J. Mechanical properties of organic semiconductors for stretchable, highly flexible, and mechanically robust electronics. *Chem. Rev.* **117** (7), 6467–6499 (2017).
8. Coropceanu, V. et al. Charge transport in organic semiconductors. *Chem. Rev.* **107** (4), 926–952 (2007).
9. Mei, J., Diao, Y., Appleton, A. L., Fang, L. & Bao, Z. Integrated materials design of organic semiconductors for field-effect transistors. *J. Am. Chem. Soc.* **135** (18), 6724–6746 (2013).
10. Anthony, J. E. The larger acenes: versatile organic semiconductors. *Chem. Rev.* **108** (11), 638–657 (2008).
11. Bronstein, H. et al. Thieno[3,2-b] thiophene-diketopyrrolopyrrole-containing polymers for high-performance organic field-effect transistors and organic photovoltaic devices. *J. Am. Chem. Soc.* **133** (10), 3272–3275 (2011).
12. Coughlin, J. E., Henson, Z. B., Welch, G. C. & Bazan, G. C. Design and synthesis of molecular semiconductors for polymer solar cells. *Acc. Chem. Res.* **47** (1), 257–270 (2014).
13. Dou, L. et al. A selenium-substituted low-bandgap polymer with improved efficiency in polymer solar cells. *Adv. Mater.* **25** (4), 6642–6648 (2012).
14. Salzner, U. & Aydin, A. The effect of donor–acceptor interactions on the electronic structure of conjugated oligomers. *J. Phys. Chem. C.* **115** (24), 11251–11267 (2011).
15. Baldo, M. A., Thompson, M. E. & Forrest, S. R. High-efficiency fluorescent organic light-emitting devices using a phosphorescent sensitizer. *Nature* **403**, 750–753 (2000).
16. Mei, J., Loth, M. A. & Bao, Z. Tailoring molecular packing and electronic properties for organic field-effect transistors. *Acc. Chem. Res.* **48** (8), 1507–1516 (2015).
17. Wang, L., Chen, X., Duan, C. & Huang, W. Effect of halogen substitution on the electronic and optical properties of organic semiconductors: A systematic review. *Prog. Mater. Sci.* **132**, 101012 (2023).
18. Fatmi, M. et al. High performance double perovskites of $cs_2inagbr_6$ and $cs_2inagcl_6$ structural electronic optical and thermoelectric properties for next generation photovoltaics. *Sci. Rep.* **15** (1), 20851 (2025).
19. Benmakhlouf, A. et al. Structural elastic and thermodynamic properties of cubic CsCl type MgCa using Ab initio approach. *Sci. Rep.* **15** (1), 1–12 (2025).
20. Djemli, A. et al. Structural, elastic, mechanic, electronic, and thermodynamic of $limon_2$ compound for electronic and energy storage. *Phys. Solid State.* **67** (5), 356–366 (2025).
21. Benamrani, A. et al. Structural, elastic, electronic, thermoelectric, and thermodynamic properties of cubic $lamgx_2$ (X = Cd, zn, Hg): For sustainable technologies. *AIP Advances* **15** (5), 055109 (2025).
22. Ghebouli, M. A. et al. Exploring the mechanical, dynamical, and thermal stability of cs_2agbix_6 (X = Br, Cl) for optoelectronic and thermoelectric applications. *Sci. Rep.* **15** (1), 20993 (2025).
23. Ghebouli, M. A., Bouferrache, K., Alanazi, F. K., Ghebouli, B. & Fatmi, M. Computational insights into the stability, mechanical, optoelectronic, and thermoelectric characteristics investigation on lead-based double perovskites of $(Cs_2, K_2, Rb_2)PbCl_6$: Promising candidates for optoelectronic applications. *Adv. Theory Simulations*. **8** (3), 2400938 (2025).
24. Bouferrache, K., Ghebouli, M. A., Ghebouli, B., Fatmi, M. & Ahmed, S. I. Correction: Organic–inorganic hexahalometalate-crystal semiconductor $K_2(Sn, Se, Te)Br_6$ hybrid double perovskites for solar energy applications. *RSC Adv.* **15** (22), 17377–17377 (2025).
25. Lee, J., Kim, K. H. & Kim, S. H. Orbital analysis and electronic structure engineering of halogenated organic semiconductors through heteroatom substitution. *Nat. Commun.* **15**, 1285 (2024).
26. Yamamoto, H., Matsumoto, T. & Takahashi, R. Spectroscopic investigations of halogen effects on optical properties of conjugated organic molecules from UV to soft X-ray energy range. *J. Phys. Chem. C.* **127** (42), 20123–20135 (2023).
27. Zhang, K., Liu, Y., Wang, L. & Chen, J. Collective excitations and plasmon resonances in halogenated organic semiconductors: implications for optoelectronic device design. *Adv. Opt. Mater.* **12** (4), 2302565 (2024).

Acknowledgements

The authors extend their appreciation to Taif University, Saudi Arabia, for supporting this work through project number (TUDSPP-2024-63).

Author contributions

Author Contribution StatementConceptualization: F. BenlakhdarData curation: M.A. Ghebouli, B. Ghebouli, S. AlomairyAnalysis: A. Djemli, Talal M. AlthagafiMethodology, Validation: M. Fatmi, Faisal KatibAlanazi.

Declarations

Competing interests
The authors declare no competing interests.

Additional information
Correspondence and requests for materials should be addressed to M.F. or F.K.A.

Reprints and permissions information is available at www.nature.com/reprints.

Publisher's note Springer Nature remains neutral with regard to jurisdictional claims in published maps and institutional affiliations.